

Review

Redox Properties of Cytochrome *c*

GIANANTONIO BATTISTUZZI, MARCO BORSARI, and MARCO SOLA

ABSTRACT

The redox properties of cytochromes (cyt) *c*, a ubiquitous class of heme-containing electron transport proteins, have been extensively investigated over the last two decades. The reduction potential (E°) is central to the chemistry of cyt *c* for two main reasons. First, E° influences both the thermodynamic and kinetic aspects of the electron exchange reaction with redox partners. Second, this thermodynamic parameter is remarkably sensitive to changes in the properties of the heme and the protein matrix, and hence can be profitably used for the investigation of the solution chemistry of cyt *c*. This research area owes much to the exploitation of voltammetric techniques for the determination of E° for metalloproteins, which dates back to the late 1970s. Since then, much effort has been devoted to the comprehension of the molecular factors that control E° in cyt *c*, which include first coordination sphere effects on the heme iron, the interactions of the heme group with the surrounding polypeptide chain and the solvent, and also include medium effects related to the nature and ionic composition of the solvent, pH, the presence of potential protein ligands, and the temperature. This article provides an overview of the most significant advances made in this field recently. *Antioxid. Redox Signal.* 3, 279–291.

INTRODUCTION

RESPIRATORY AND PHOTOSYNTHETIC PROCESSES include multistep thermodynamically driven electron transport chains that involve multisubunit protein complexes anchored to the cell membrane, containing a variety of metal redox cofactors, and mobile electron carriers that shuttle electrons among the former species (29, 40). These electron carriers may consist of organic molecules (for example, the ubiquinone/ubihydroquinone system) or small metalloproteins ($M_r = 10\text{--}15$ kDa), such as cytochromes *c* (cyt), blue copper proteins, and iron-sulfur proteins (29, 40).

Considerable effort has been devoted to the elucidation of the molecular details of biological electron transport, which is still one of the leading areas of biophysical research (40). In

this context, the comprehension of the molecular determinants of the reduction potential (E°) of the redox centers involved in the electron transfer chains appears to be of paramount importance. In fact, the E° values determine the direction of the electron flow and control the driving force of each electron transfer step (53), thereby influencing both the thermodynamic and kinetic aspects of the process. The reduction potential reflects the relative stability of the oxidized and reduced forms of the metalloprotein and is the result of a delicate interplay between the properties of the metal center and those of the polypeptide chain (29, 40, 55, 59). Any alteration of this equilibrium modifies the E° value of the protein and may therefore heavily affect its functional properties.

Cyt *c* are by far the most thoroughly characterized electron transfer metalloproteins, due

to their diffusion (they are present virtually in all living systems), stability, and ease of purification (13, 40, 59, 63, 70). These species are monomeric heme proteins in which the heme group(s) is covalently linked to the polypeptide chain through two thioether bonds involving two cysteines and two axial ligands to the iron (either His, Met or His, His). Cyt *c* are grouped into four subclasses on the basis of their structural properties (59). The most widely studied species belong to class I, found in both eukaryotes and prokaryotes, which feature a low-spin six-coordinate heme iron possessing a His-Met axial coordination, which constitute the main focus of this article, and to class III, which are multiheme proteins with bishistidinyl coordination of bacterial origin (59, 63, 70). Classes II and IV include cyt *c'*, in which the heme iron is high-spin pentacoordinate with an axial histidine ligand, and bacterial tetraheme proteins containing bis-His and His-Met coordinated heme, respectively (59).

Class I cyt *c*, which participate in mitochondrial respiration and bacterial photosynthesis and are involved in several metabolic pathways, contain a single heme near the N-terminus with a histidine and a methionine residue acting as axial iron ligands (Fig. 1). These small globular proteins ($M_r = 10\text{--}15$ kDa) are highly

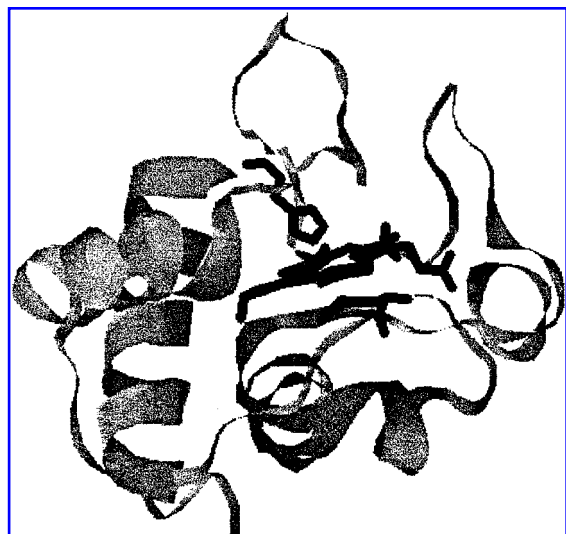


FIG. 1. Ribbon view of horse heart cyt *c* (8) showing the iron axial ligands (His¹⁸ and Met⁸⁰) and the thioether bonds (involving Cys¹⁴ and Cys¹⁷).

basic and show a quite conserved polypeptide folding. The heme is surrounded by a hydrophobic environment and is exposed only slightly to the solvent ($\sim 4\%$). These features contribute to the quite positive reduction potentials of these species (59), which place them at the upper end of the electron transfer chains, and prevent formation of oxo-ferryl species typical of redox heme-enzymes, as cyt P_{450} , peroxidases, and catalases. Cyt *c* from photosynthetic bacteria, generally indicated as cyt c_2 , act as electron donors to the photooxidized photosynthetic reaction center, whereas the mitochondrial proteins shuttle electrons between the last two membrane-bound components of the electron transfer chain of oxidative phosphorylation, namely, ubiquinol-cyt *c* reductase (complex III, $M_r = 150$ kDa) and cyt *c* oxidase (complex IV, $M_r = 200$ kDa) (13, 40, 59, 70).

Mitochondrial cyt *c* acts also as a key regulator in apoptosis, the programmed cell death (47, 57, 80). After its release from the mitochondrial periplasmic space into the cytosol, cyt *c* forms a protein complex with Apaf-1, caspase-9, and ATP, called apoptosome, which activates the degradation phase of apoptosis (47, 48, 57, 64, 80). Apparently, this process does not imply any electron transfer, because Zn- and Cu-substituted cyt *c*, which are redox-inactive, are as effective as native cyt *c* in forming apoptosomes (49, 64). However, it is worthy of note that the release of cyt *c* from the mitochondrial periplasmic space leads irreversibly to cell death, either by apoptosis or by necrosis, due to the inactivation of the electron transfer chain involved in respiration, which prevents ATP synthesis and induces the formation of dangerous radical species, such as superoxide (47, 48, 57, 80). Cyt *c* therefore exerts an important antioxidant action by indirectly controlling the amount of superoxide anion produced at the ubiquinone site of ubiquinol-cyt *c* reductase (complex III) (57) and by participating in the reduction of the potentially dangerous hydrogen peroxide catalyzed by the redox enzyme cyt *c* peroxidase, one of its physiological redox partners (29, 40, 59, 70). The analysis of the interaction between mitochondrial cyt *c* and the latter protein provided much of the present knowledge about the mechanism of electron

exchange in biological systems (40, 59, 70). The electron transfer reaction between the two proteins is a collision-dependent process involving the formation of transient protein–protein complexes (62) stabilized by highly specific electrostatic interactions between regions of opposite charge, in which the positively charged domain formed by the clustered lysines surrounding the exposed heme edge of cyt *c* plays a key role (56, 62, 83). Fast electron transfer occurs within the complex, which immediately dissociates thereafter (58). The rate of the overall electron transfer reaction depends on a number of variables, such as the distance and the reciprocal orientation of the redox centers, the nature of the intervening polypeptide matrix, the difference between the reduction potentials of the two metal centers, and the properties of the solvent, which remarkably influence the formation of the protein–protein complex (30, 40, 58, 82).

DIRECT ELECTROCHEMISTRY OF CYT *c*

The kinetics of heterogeneous electron transfer between proteins and bare electrodes is, in general, too slow to allow a successful application of direct electrochemistry techniques (cyclic voltammetry and square wave voltammetry), at variance with that of simple coordination compounds and organic molecules. The most severe obstacle is the denaturing adsorption of protein molecules onto the electrode surface, which leads to the formation of a sort of nonconducting film that prevents the electron exchange of the freely diffusing species (2). Other disfavoring factors are related to the low diffusion coefficients of proteins due to the high molecular mass, the burial of the metal center within the protein matrix, and the absence of surface-specific interactions, which instead occur between biological redox partners.

These problems were brilliantly solved for class I cyt *c* at the end of the 1970s, with the introduction of solid electrodes functionalized with promoters (34, 35). Promoters are organic molecules with a rigid conjugated structure that strongly adsorb on the electrode surface in a monolayer. In this way, they prevent protein

denaturation and, interacting transiently with some part of the protein surface, help the correct orientation of the molecule to be obtained, which allows for fast electron transfer with the solid electrode (27, 42, 44). Therefore, the overall effect of promoters is to facilitate electron transfer between the redox center of the protein and the electrode, without being involved in the redox reaction itself (27, 42, 44). The feasibility of direct electrochemistry at solid electrodes (Fig. 2) [which is now possible for electron transport metalloproteins and redox enzymes with molecular masses up to ~200 kDa (3, 4, 44)] opened the way to the detailed characterization of the redox properties of class I cyt *c* and to the comprehension of the factors influencing it at a molecular level. In fact, the application of time-resolved voltammetric techniques allows insight to be gained on both the thermodynamic and kinetic aspects of the

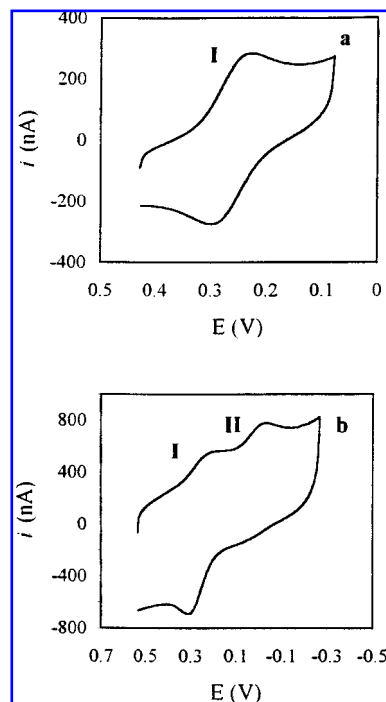


FIG. 2. Cyclic voltammograms of beef heart cyt *c* at a 4-mercaptopyridine surface-modified gold disc electrode. (a) pH 6.95, (b) pH 9.13. Conditions were as follows: temperature, 293 K; base electrolyte, 0.1 M sodium acetate; scan rate, 50 mV/s⁻¹. I and II refer to the waves of the native and alkaline conformer, respectively. Reprinted by permission from Battistuzzi *et al.* *Biochemistry* 38: 7900–7907, 1999. Copyright 1999 American Chemical Society.

electron transfer process and of coupled chemical reactions involving one or both redox states, such as acid–base and conformational equilibria (14, 16, 20–22, 24, 36). Moreover, variable-temperature $E^{\circ'}$ measurements allows determination of the enthalpy and entropy changes associated with the reduction process (19, 21, 24–26, 46, 50, 51, 76, 77), which are of use for the characterization of the determinants of the reduction potential of these species (see below).

THE REDUCTION POTENTIAL OF CLASS I CYT *c*

The $E^{\circ'}$ values of class I cyt *c* vary from +0.2 to +0.35 V (versus saturated hydrogen electrode) (59). A significant contribution to these high reduction potentials arises from the π -electron acceptor character of the thioether sulfur atom of the methionine axially bound to the iron, which stabilizes the reduced (+2) state. Redox studies of a heme octapeptide (a proteolytic fragment of cyt *c* retaining the heme and the axial histidine in which the second axial position can be occupied by various ligands) (78) and of model porphyrin complexes (52) show indeed that His–Met axial coordination induces an increase in $E^{\circ'}$ of ~ 0.16 V as compared with bis-His coordination, typical of the multiheme class III cyt *c*. The $E^{\circ'}$ values for the latter species fall in the range from -0.4 to -0.1 V. Hence, this exquisitely coordinative effect accounts *per se* for about one third of the difference between the redox potentials of these classes of cyt *c* (59).

The electrostatic interactions of the charge of the redox center with buried and surface charges, polar groups of the protein, and solvent dipoles are additional important effectors of $E^{\circ'}$ (40, 41, 55, 59, 70, 78, 79). In particular, the poor accessibility of the heme to the solvent and the burial of the heme within a hydrophobic pocket induce a significant enthalpic stabilization of the ferrous over the ferric state, thus contributing to the high redox potential of cyt *c* (19). The hydrophobicity of the heme environment should strengthen the electrostatic interactions between the redox center and the polar and charged groups within the protein (41,

55, 78, 79), whereas the electrostatic effect of the net or fractional charges on the protein surface should be quenched by the high dielectric constant of water. The question of how and to what extent these interactions control $E^{\circ'}$ in cyt *c* has attracted the interest of many workers, who addressed the problem with theoretical and experimental approaches (59). The former focused mainly on the development of models for the calculation of the electrostatic interaction energies of the heme with polar and charged residues and solvent dipoles able to reproduce the differences in $E^{\circ'}$ among different cyt *c* (28, 66, 79). The latter, which involved experiments of chemical modification, site-directed mutagenesis, and specific anion binding, sought to quantify the effects exerted on the $E^{\circ'}$ value by internal or surface charges (15, 17, 18, 31, 59, 65). Evidence has been obtained that the alteration of internal net charges of cyt *c*, such as the heme propionates, induces variations in $E^{\circ'}$ (50–65 mV) that are more pronounced than those due to surface charges (5–15 mV). The overall effect depends on several factors, such as the heme–charge distance and the dielectric properties of the intervening medium, which can be described by an “effective dielectric constant,” which is different for each particular interaction and involves contributions from both the solvent and the protein (15, 17, 18, 55, 59, 65).

A further important contribution to the reduction potential of class I cyt *c* originates from the differences in dynamic and solvation properties between the two redox states. In fact, it is recognized that solvent reorganization effects and changes in protein flexibility, the latter intended as the sum of the conformational (vibrational, torsional) degrees of freedom, associated with reduction of cyt *c* play a major role in determining the entropic contribution to $E^{\circ'}$ (6–9, 12, 13, 19–21, 24, 25). Reduction turns out to be invariably disfavored on entropic grounds ($\Delta S_{rc}^{\circ'} < 0$) (19, 26): although this is consistent with the decreased flexibility of the reduced state as compared with the ferri form determined by nuclear magnetic resonance in solution (8–12), the reduction-induced changes in the H-bonding network within the hydration sphere of the molecule that contribute to the entropy loss are still largely uncharacterized.

The entropic term strongly affects $E^{\circ'}$ (19). Nevertheless, this term is most often neglected in the discussions concerning the determinants of the differences in $E^{\circ'}$ among cyt *c* from different sources, which focus solely on electrostatic and coordinative effects, which are exquisitely enthalpic effects.

Many of the contributions to $E^{\circ'}$, such as the differences in solvation properties between the two redox forms, the electrostatic interactions at the heme-protein/solvent interface, and even axial coordination to the heme iron, are strongly influenced by the pH, ionic composition, and dielectric constant of the solvent. These effects are particularly relevant from the physiological point of view: they clearly indicate that the function of cyt *c* is strongly affected by the properties of the environment, which consequently plays a major role in the control of the biological electron transfer reactions *in vivo* (40, 59).

pH DEPENDENCE OF E°

The polypeptide folding, the electronic distribution onto the heme, axial heme ligation and, consequently, the redox potential of class I cyt *c* are sensitive to acid–base equilibria involving ionizable groups such as the axial ligands, the heme propionates, and distal residues (16, 21, 59, 60, 70). At least five pH-dependent conformational states have been characterized for the ferri form (49). For example, the native His,Met-ligated form (state III) originates a low-pH conformer (state II, with an apparent pK_a of 2.5) in which the axial ligands are protonated and detached from the iron, which becomes high spin, and are likely substituted by water molecules. The $E^{\circ'}$ of this form (which is expected to be remarkably high) cannot be detected owing to the worsening of the electrochemical response at low pH caused by the protonation of the promoter and the likely disruption of the adsorbed layer (16). At alkaline pH values, state III undergoes a transition to an “alkaline conformer” (state IV, with apparent pK_a of ~ 9), which involves replacement of the axial methionine with an endogenous ligand, most probably a lysine. This conformer is characterized by a negative potential (see be-

low). Upon increasing the pH above 10, another state (state V) becomes accessible, in which probably a hydroxide ion is axially bound to the heme iron (32).

The potential of native cyt *c* (state III) is also sensitive to acid–base equilibria due to residues such as the heme propionates or distal histidines (55, 59) (Fig. 3). The deprotonation of an ionizing residue induces a decrease in $E^{\circ'}$ because of the electrostatic stabilization of the oxidized form due to the decrease of the overall positive charge of the protein. The extent of the $E^{\circ'}$ change depends on the solvation properties of the residue, the distance from the heme, and the properties of the intervening medium. The pH dependence of $E^{\circ'}$ has a typical sigmoidal shape, which can be fitted by the equation:

$$E^{\circ'} = E_a^{\circ'} - 2.303 \cdot \frac{RT}{nF} \cdot \log \frac{[H^+] + K_{ox}}{[H^+] + K_{red}} \quad (1)$$

in which $E_a^{\circ'}$ is the limit $E^{\circ'}$ value for the protein containing the ionizing residue in the fully

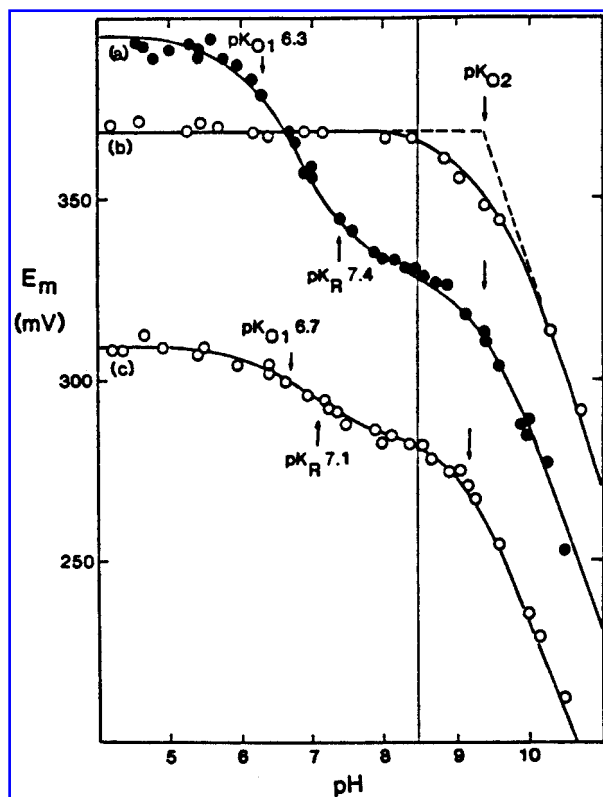


FIG. 3. pH dependence of the redox potential of cyt *c*₂ from (a) *Rm. vannielii*, (b) *Rps. viridis*, and (c) *Rb. capsulatus*. Reprinted by permission from Moore GR, and Pettigrew GW. *Cytochromes c: Evolutionary, Structural and Physicochemical Aspects*. Berlin: Springer-Verlag, 1990.

protonated form, and K_{ox} and K_{red} are the proton dissociation constants for the oxidized and reduced protein, respectively (33, 59, 60). This equation is based on the higher proton affinity of reduced cyt *c* as compared with the oxidized form, owing to its lower positive charge. As a consequence, whereas at extreme pH values the residue involved in the proton equilibrium is protonated or deprotonated in both redox states, at intermediate pH values it is protonated mainly in the reduced form. This approach has a general validity and can be extended also to more complex situations involving multiple acid–base equilibria (59).

The moderate affinity of the axial methionine sulfur for the ferric ion in the native form of cyt *c* (state III) renders this residue susceptible to substitution by endogenous ligand(s) at high pH, leading to the “alkaline” isomer(s) (state IV), in which the iron retains the low-spin ferric state (14, 16, 19–22, 24, 32, 37, 45, 59, 67, 70, 75). The spectroscopic and redox changes induced by this equilibrium have been exploited to determine the thermodynamics and kinetics of the isomerization, to identify the nature of the substituting ligands, and to determine the role of the residues neighboring the heme in the relative stabilization of the two conformers. The overall reaction turns out to be a two-step process in which a fast residue deprotonation triggers a slow and thermodynamically favored conformational change that leads to the replacement of the methionine by a surface lysine as heme axial ligand, with an apparent pK_a in the range 8.5–9.5, depending on the species (59, 70). The ionizing residue has not been unambiguously identified yet, and no detailed information is available on the structural features of the alkaline conformers. The existence of two alkaline isomers in a pH dependent ratio suggests that at least two lysine residues can substitute for the methionine at high pH (19, 21, 22, 32, 37, 45, 67).

The alkaline isomerization has a dramatic effect on the redox properties of cyt *c*. In fact, the reduction potential of the alkaline isomers for various species is lower than that of the native form by 0.3–0.5 V (falling in the range -0.05 V to -0.15 V) (14, 16, 20–22, 24, 42) (Fig. 2). It has been found that this remarkable difference is mainly due to the different coordination prop-

erties of the native methionine and the substituting lysine: the latter is a stronger donor ligand that selectively stabilizes the ferri form, thereby inducing a remarkable decrease in the redox potential (19).

The alkaline transition is greatly influenced by the temperature and the properties of the medium. This isomerization turns out to be endothermic (22). Therefore, the pK_a decreases with increasing temperature (Fig. 4). This effect is particularly relevant for cyt *c* from plants and photosynthetic bacteria for which the alkaline isomer appears at pH values as low as 7 upon increasing the temperature above $\sim 40^\circ\text{C}$ (33). The pK_a also decreases with decreasing dielectric constant of the medium, as noted in mixed water/dimethyl sulfoxide solutions (20). This effect is of potential relevance from a physiological point of view because it has been reported that a decrease of the dielectric constant occurs near the surface of phospholipid membranes and that the alkaline form of cyt *c* is involved in the interaction with synthetic anion phospholipid vesicles (72–74). Interestingly, monoclonal antibody binding studies indicate that only the native form is present in live cells,

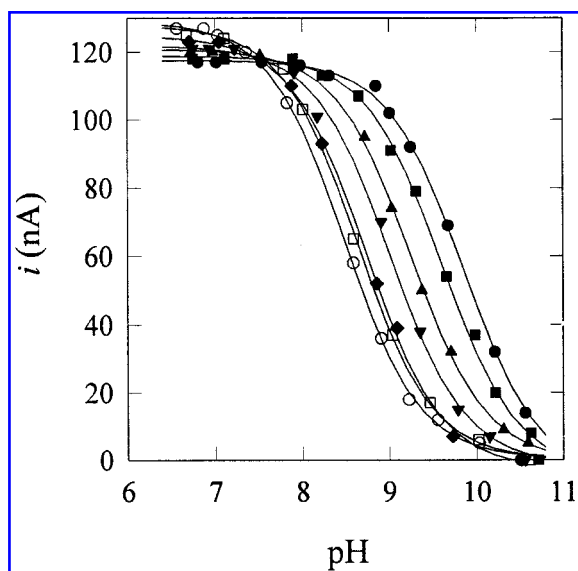


FIG. 4. pH dependence of the current intensity of the cathodic peak (*i*) of wave I for beef heart cyt *c* at different temperatures in sodium acetate at $I = 0.1$ M. Temperatures are 5°C (●), 10°C (■), 20°C (▲), 30°C (▼), 40°C (◆), 50°C (□), and 60°C (○). Reprinted by permission from Battistuzzi *et al. Biochemistry* 38: 7900–7907, 1999. Copyright 1999 American Chemical Society.

where cyt *c* acts as an electron shuttle near the inner mitochondrial membrane, whereas the presence of the alkaline isomers has been clearly detected in apoptotic and necrotic cells (47). The alkaline isomers are formed in the early stages of apoptosis and necrosis, possibly as a result of the translocation of cyt *c* through the mitochondrial membrane (or of its association with membranes altered during the death process). It is therefore possible that the phospholipid-induced conformational changes associated with the formation of the alkaline isomers are connected with the signaling role of cyt *c* during apoptosis, although experimental evidence seems to indicate that these isomers are not involved in the interaction with Apaf-1 to form apoptosomes (47, 64).

Finally, the pK_a increases with increasing ionic strength (22). This is likely one of the factors that hamper separation of the alkaline form in the crystal state from the usual high-ionic strength solutions (ammonium sulfate) used in the crystallization procedure.

IONIC STRENGTH AND SPECIFIC ION BINDING EFFECTS ON $E^{\circ'}$

The ionic composition of the medium affects significantly the reactivity of cyt *c*. In particular, it influences the interactions with the redox partners (58) and phospholipid membranes (43). But salt effects also modulate the reduction potential of cyt *c*. Two main effects can be recognized. The first is the general ionic strength effect that alters the activity coefficients of both redox forms. The second is due to specific protein–anion interactions at surface sites (cyt *c* is positively charged at neutral pH). The former effect causes a decrease in $E^{\circ'}$ because of the stabilization of the oxidized form (which carries the larger positive charge) due to the shielding of the surface charges of the protein by the surrounding “ionic atmosphere.” With the assumption that the protein behaves as a low dielectric cavity carrying a net charge uniformly distributed on the surface, and combining the Nernst and extended Debye–Huckel equations, Margalit and Schejter obtained the following expression for the

changes in $E^{\circ'}$ of cyt *c* induced by the ionic atmosphere, in the absence of specific ion–protein interactions (38, 54, 59):

$$E^{\circ} = E_{I=0}^{\circ} + 2.303 \cdot \frac{RT}{nF} \cdot \left(z_{\text{red}}^2 - z_{\text{ox}}^2 \right) \cdot \frac{0.5 \cdot \sqrt{I}}{1 + 0.33 \cdot A \cdot \sqrt{I}} \quad (2)$$

where I is the ionic strength, $E_{I=0}^{\circ}$ is the redox potential extrapolated at zero ionic strength, z_{red} and z_{ox} are the charges of the reduced and oxidized proteins, respectively, and A is the “ion-size parameter,” defined as the mean distance of closest approach between the protein and an ion of opposite charge belonging to the ionic atmosphere. The value of A is comprised of the sum of the crystallographic radii and the sum of the solvated radii. An A value of 18 Å has been used for bovine ferricytochrome *c*. By assuming

$$f(I) = (0.5\sqrt{I}) / (1 + 0.33 \cdot A \cdot \sqrt{I}) \quad (3)$$

Eq. 2 becomes:

$$E^{\circ} = E_{I=0}^{\circ} + 0.059(z_{\text{red}}^2 - z_{\text{ox}}^2)f(I) \quad (4)$$

which predicts a linear decrease in E° with increasing $f(I)$, with a slope given by $0.059(z_{\text{red}}^2 - z_{\text{ox}}^2)$. Despite the roughness of the model, especially regarding the dielectric properties of the protein medium, this approach proved to be surprisingly effective in describing the ionic strength dependence of E° for native and chemically modified class I cyt *c* (5, 15, 17, 18, 22, 24, 38, 39, 54, 69).

The analysis of the thermodynamics of the redox reaction of mitochondrial cyt *c* in the presence of increasing concentrations of non-binding anions allowed further insight to be gained into the effect of the “ionic atmosphere” on $E^{\circ'}$ (24). In particular, it has been found that: (i) the moderate decrease in $E^{\circ'}$ observed with increasing ionic strength is mainly due to the stabilizing enthalpic effect that the negatively charged ionic atmosphere exerts on the ferri form; and (ii) in the absence of the screening effects of the salt ions on the network of the electrostatic interactions at the protein–solvent interface, the solvation properties and the con-

formational flexibility of the two redox states are comparable, because the reduction entropy extrapolated at null ionic strength is approximately zero.

Specific anion-binding to one or both redox forms of the protein alters the net charges, inducing a change in the slope of $E^{\circ'}$ versus $f(I)$ as compared with the free protein. These changes have been exploited to determine the stoichiometry of specific ion-protein interactions for a wide variety of biologically relevant anions (15, 17, 18). Several showed peculiar binding properties, often including sequential anion binding due to the presence of multiple binding sites (1, 61) with different affinities for the anion. Comparison of anion binding data for a number of class I cyt *c* indicates that several anion binding sites are conserved in proteins from different sources, also with low sequence identity. This is in agreement with the existence of regions of relatively conserved electrostatic potential in these species, which are most likely those involved in the interaction with physiological partners (54).

As nuclear magnetic resonance and x-ray data clearly indicate that increasing anion concentrations induce only minor structural modifications, which leave the overall protein folding and conformational flexibility of the molecule largely unaffected (9, 68), it is reasonable to assume that the modification of $E^{\circ'}$ caused by specific anion binding is mainly electrostatic in origin, due to the partial neutralization of positive surface charges. Therefore, the difference between the $E^{\circ'}$ value extrapolated at $f(I) = 0$ ($E^{\circ}_{I=0}$) in the presence of anions forming a 1:1 complex with both redox forms of the protein (which corresponds to the $E^{\circ'}$ of a protein whose overall charge is decreased by that of the bound anion) and that of the anion-free protein yields an estimate of the decrease in redox potential due to the neutralization of a number of positive charges equal to that of the bound anion. The data obtained indicate that neutralization of a net surface charge due to anion binding induces a decrease in $E^{\circ'}$ of ~ 15 – 20 mV (15, 17, 18), which is a value quite similar to those obtained previously for mutated or chemically modified cyt *c* (55, 59).

TEMPERATURE DEPENDENCE OF $E^{\circ'}$

Temperature strongly affects the redox behavior of class I cyt *c*. The reduction potential of class I cyt *c* invariably decreases with increasing temperature between 5 and 65°C. However, the temperature profile of $E^{\circ'}$ is pH-dependent and differs slightly for species from different sources (19–21, 24–26, 46, 50, 51, 76, 77). In particular, the $E^{\circ'}$ of the native His,Met-ligated form of cyt *c* from mammalian mitochondria shows a monotonic linear decrease with increasing temperature at slightly acidic and neutral pH values, whereas at higher pH values the $E^{\circ'}$ versus temperature plot becomes clearly biphasic with a transition point at $\sim 50^{\circ}\text{C}$ (Fig. 5). This behavior has been ascribed to a reversible nonequilibrium conformational transition between two states of the oxidized native form, which implies a fractional loss of proton on passing from the low-temperature to the high-temperature conformer (46). The decrease of the temperature of the break in the $E^{\circ'}$ /temperature profile with increasing pH is consistent with this proposal (19). Spectroscopic studies indicate that the low- and high-temperature native conformers do not differ significantly in the surroundings of the heme (19). The temperature profiles of $E^{\circ'}$ for class I cyt *c* from plant mitochondria and photosynthetic bacteria are similar to the above, but show some significant differences (19, 21). In particular: (i) the transition between the low- and the high-temperature native forms occurs at lower pH values and lower temperatures (35–40°C); (ii) the temperature of the transition point sensibly decreases with increasing pH; and (iii) the temperature-induced decrease in the pK_a for the alkaline transition is greater as compared with that in their mammalian analogues.

An additional effect of increasing temperature is the depression of the pK_a for the alkaline transition, as mentioned above.

The temperature dependence of the $E^{\circ'}$ of cyt *c* allows determination of the thermodynamic parameters of the electron transfer process. In particular, the use of nonisothermal electrochemical cells, in which the reference electrode (saturated calomel electrode) is kept at constant

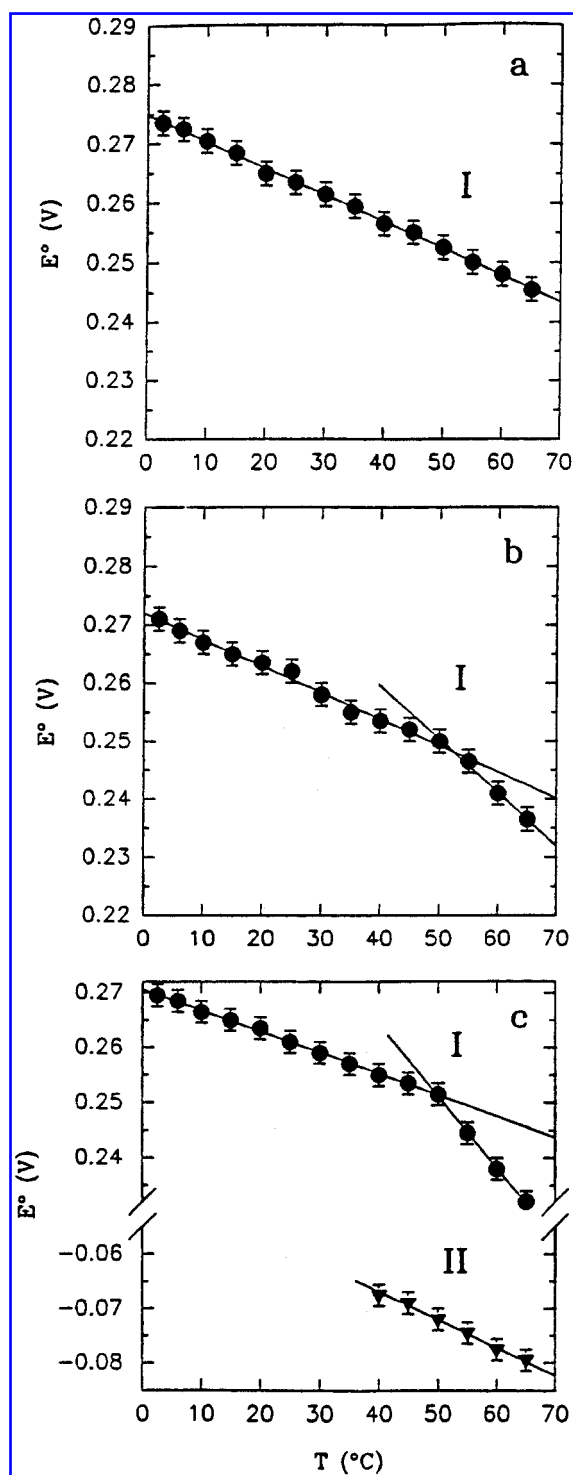


FIG. 5. Temperature dependence of the reduction potential of beef heart cyt *c* at pH 6.9 (a), pH 7.5 (b), and pH 8.3 (c). Base electrolyte was 0.1 M sodium chloride. Solid lines are least-squares fits to the data points. I and II refer to the waves of the native and alkaline conformer, respectively. Reprinted by permission from Battistuzzi *et al.* *Biochemistry* 36: 16247–16258, 1997. Copyright 1997 American Chemical Society.

temperature, whereas the half-cell containing the working electrode is kept under thermostatic control (81), allows the standard entropy (ΔS_{rc}°) and enthalpy (ΔH_{rc}°) changes associated with reduction of the oxidized protein to be determined directly from the slope of the plots of E° versus temperature and of E°/T versus $1/T$, respectively (19, 21, 24–26, 46, 50, 51, 76, 77). The analysis of the thermodynamic parameters of protein reduction for mitochondrial and bacterial class I cyt *c* (Table 1), carried out in the light of the extensive information on their structural and dynamic properties, allowed further insight to be gained into the factors affecting the reduction potential. The picture that comes out is that the high redox potential of these proteins has mainly an enthalpic origin, due to the stabilization of the ferroheme by ligand binding interactions and the hydrophobicity of the heme environment (19–21, 24). The entropic term, which is linked to solvation and dynamic properties of the molecule, instead invariably disfavors protein reduction and tends to lower the E° values. Although smaller than the enthalpic term, ΔS_{rc}° plays an important role in the modulation of the reduction potential in these species (19–21, 24). A similar balance between the enthalpic and entropic contributions to E° has been determined for all the other classes of high-potential metalloproteins, namely, blue copper proteins and high potential iron-sulfur proteins (23, 71). Therefore, it is apparent that nature uses the same strategy to control the redox potential of these species for reasons that are still unclear and that constitute a fascinating field for future investigations.

The comparison of the ΔS_{rc}° and ΔH_{rc}° values for the native and the alkaline isomers of class I cyt *c* clearly indicates that the difference between their redox potentials is almost entirely an enthalpic effect, consistent with the stronger donor properties of the substituting lysine as compared with the native methionine (19, 22).

CONCLUDING REMARKS

The E° of cyt *c*, as that of any other electron transport metalloprotein, is determined by: (i) bonding interactions at the metal center; (ii)

TABLE 1. $E^{\circ'}$, $\Delta H_{rc}^{\circ'}$, AND $\Delta S_{rc}^{\circ'}$ VALUES FOR THE NATIVE AND ALKALINE FORMS OF SELECTED CLASS I CYT *c*

Cyt <i>c</i>	<i>pH</i>	$E_N^{\circ'}$	$E_A^{\circ'}$	$\Delta S_{rc}^{\circ'}$		$\Delta H_{rc}^{\circ'}$	
				<i>Native</i>	<i>Alkaline</i>	<i>Native</i>	<i>Alkaline</i>
Beef heart	6.9	+0.263		−44		−38	
	7.5	+0.262		−43		−38	
				−96		−55	
	8.3	+0.261	−0.075	−37	−50	−36	−9
Spinach				−125		−65	
	7.0	+0.268		−29		−35	
				−58		−43	
	7.5	+0.268	−0.112	−27	−33	−34	+1
				−58		−43	
Cucumber	8.4	+0.267	−0.121	−20	−40	−32	0
				−58		−43	
	7.0	+0.271		−23		−33	
				−58		−44	
	7.5	+0.270	−0.164	−19	−38	−32	+4
Sweet potato				−64		−46	
	8.5	+0.268	−0.173	−13	−41	−30	+4
				−64		−46	
	7.0	+0.274		−31		−36	
				−77		−50	
<i>Rps. palustris</i> cyt <i>c</i> ₂	7.6	+0.274	−0.145	−24	−41	−34	+2
				−79		−51	
	8.4	+0.272	−0.153	−17	−47	−31	+1
				−106		−59	
	7	+0.362		−67	−62	−55	−14
<i>Rb. sphaeroides</i> cyt <i>c</i> ₂				−151		−81	
	8.5	+0.359	−0.056	−60	−62	−52	−13
				−152		−80	
	7	+0.354		−69	−63	−55	−13
				−152		−81	
<i>Rb. capsulatus</i> cyt <i>c</i> ₂	9	+0.353	−0.054	−63	−61	−53	−13
				−154		−82	
	7	+0.347		−66	−60	−52	−9
				−94		−61	
	9	+0.345	−0.095	−58	−61	−50	−9
				−89		−60	

$E^{\circ'}$ (V), $\Delta H_{rc}^{\circ'}$ (kJ/mol), and $\Delta S_{rc}^{\circ'}$ (J/mol/K) values for the native (N) and alkaline (A) forms of selected class I cyt *c* are presented. The $\Delta S_{rc}^{\circ'}$ and $\Delta H_{rc}^{\circ'}$ values for the native species in the upper and lower rows refer to the low- and high-temperature conformers, respectively. The temperature was 25°C. Data are taken from references 19 and 21.

electrostatic interactions between the redox center and buried and surface net charges, polar groups within the protein, and solvent dipoles; (iii) the binding of exogenous ligands to the protein (*i.e.*, protons or ions); and (iv) the conformational differences between the two redox forms of the protein (affecting mainly the entropic term). Direct electrochemistry at solid electrodes proved to be a valuable tool for addressing the problem of the relationships of the redox properties of cyt *c* with structural features [especially in combination with site-directed mutagenesis techniques that provides a virtually infinite number of proteins with sin-

gle and multiple-point mutations in selected positions (55)], nature of the medium and temperature. The thermodynamic and kinetic data ($E^{\circ'}$, $\Delta S_{rc}^{\circ'}$, and $\Delta H_{rc}^{\circ'}$ values and rate constants of reactions coupled with the electron transport) obtained with these techniques, interpreted with the aid of the structural information provided by the modern techniques of structural biology and computer chemistry, constitute an important resource to improve our understanding of the factors affecting the redox properties, hence the biological function, of these ubiquitous electron transport metalloproteins.

ACKNOWLEDGMENTS

This work was performed with the financial support of the Ministero dell'Università e della Ricerca Scientifica e Tecnologica of Italy (Programmi di Ricerca Scientifica di Rilevante Interesse Nazionale, PRIN 98) and the Consiglio Nazionale delle Ricerche of Italy.

ABBREVIATIONS

cyt, cytochrome(s); E° , reduction potential; ΔH° , standard enthalpy change; ΔS° , standard entropy change.

REFERENCES

1. Arean CO, Moore GR, Williams G, and Williams RJP. Ion binding to cytochrome *c*. *Eur J Biochem* 173: 607–615, 1988.
2. Armstrong FA. Probing metalloproteins by voltammetry. *Struct Bonding* 72: 137–222, 1990.
3. Armstrong FA, Butt JN, and Sucheta A. Voltammetric studies of redox-active centers in metalloproteins adsorbed on electrodes. *Methods Enzymol* 227: 479–500, 1993.
4. Armstrong FA, Heering HA, and Hirst J. Reaction of complex metalloproteins studied by protein-film voltammetry. *Chem Soc Rev* 26: 169–179, 1997.
5. Aviram I, Myer YP, and Schejter A. Stepwise modification of the electrostatic charge of cytochrome *c*. *J Biol Chem* 256: 5540–5544, 1981.
6. Baistrocchi P, Banci L, Bertini I, Turano P, Bren KL, and Gray HB. Three-dimensional solution structure of *Saccharomyces cerevisiae* reduced iso-1-cytochrome *c*. *Biochemistry* 35: 13788–13796, 1996.
7. Banci L, Bertini I, Bren KL, Gray HB, Sompornpisut P, and Turano P. Solution structure of oxidized *Saccharomyces cerevisiae* iso-1-cytochrome *c*. *Biochemistry* 36: 8992–9001, 1997.
8. Banci L, Bertini I, Gray HB, Luchinat C, Redding T, Rosato A, and Turano P. Solution structure of oxidized horse heart cytochrome *c*. *Biochemistry* 36: 9867–9877, 1997.
9. Banci L, Bertini I, Redding T, and Turano P. Monitoring the conformational flexibility of cytochrome *c* at low ionic strength by ^1H -NMR spectroscopy. *Eur J Biochem* 256: 271–278, 1997.
10. Banci L, Gori-Savellini G, and Turano P. A molecular dynamics study in explicit water of the reduced and oxidized forms of yeast iso-1-cytochrome *c*. *Eur J Biochem* 249: 716–723, 1997.
11. Banci L, Bertini I, Spyroulias GA, and Turano P. The conformational flexibility of oxidized cytochrome *c* studied through its interaction with NH_3 and at high temperatures. *Eur J Inorg Chem* 583–591, 1998.
12. Banci L, Bertini I, Huber JG, Spyroulias GA, and Turano P. Solution structure of reduced horse heart cytochrome *c*. *J Biol Inorg Chem* 4: 21–31, 1999.
13. Banci L, Bertini I, Rosato A, and Varani G. Mitochondrial cytochromes *c*: a comparative analysis. *J Biol Inorg Chem* 4: 824–837, 1999.
14. Barker PD, and Mauk AG. pH-linked conformational regulation of a metalloprotein oxidation–reduction equilibrium: electrochemical analysis of the alkaline form of cytochrome *c*. *J Am Chem Soc* 114: 3619–3624, 1992.
15. Battistuzzi G, Borsari M, Dallari D, Ferretti S, and Sola M. Cyclic voltammetry and ^1H NMR of *Rhodopseudomonas palustris* cytochrome *c*₂. Probing the chemistry of surface charges through anion binding studies. *Eur J Biochem* 233: 335–339, 1995.
16. Battistuzzi G, Borsari M, Ferretti S, Sola M, and Soliani E. Cyclic voltammetry and ^1H NMR of *Rhodopseudomonas palustris* cytochrome *c*₂. pH dependent conformational states. *Eur J Biochem* 232: 206–213, 1995.
17. Battistuzzi G, Borsari M, Dallari D, Lancellotti L, and Sola M. Anion binding to mitochondrial cytochromes *c* studied through electrochemistry. Effects of the neutralization of surface charges on the redox potential. *Eur J Biochem* 241: 208–214, 1996.
18. Battistuzzi G, Borsari M, and Sola M. Anion binding to cytochrome *c*₂. Implications on protein-ion in class I cytochromes *c*. *Arch Biochem Biophys* 339: 283–290, 1997.
19. Battistuzzi G, Borsari M, Sola M, and Francia F. Redox thermodynamics of the native and alkaline forms of eukaryotic and bacterial class I cytochromes *c*. *Biochemistry* 36: 16247–16258, 1997.
20. Battistuzzi G, Borsari M, Rossi G, and Sola M. Effects of solvent on the redox properties of cytochrome *c*: cyclic voltammetry and ^1H NMR experiments in mixed water–dimethylsulfoxide solutions. *Inorg Chim Acta* 272: 168–175, 1998.
21. Battistuzzi G, Borsari M, Cowan JA, Eicken C, Loschi L, and Sola M. Redox chemistry and acid–base equilibria of mitochondrial plant cytochromes *c*. *Biochemistry* 38: 5553–5562, 1999.
22. Battistuzzi G, Borsari M, Loschi L, Martinelli M, and Sola M. Thermodynamics of the alkaline transition of cytochrome *c*. *Biochemistry* 38: 7900–7907, 1999.
23. Battistuzzi G, Borsari M, Loschi L, Righi F, and Sola M. Redox thermodynamics of blue copper proteins. *J Am Chem Soc* 121: 501–506, 1999.
24. Battistuzzi G, Borsari M, Loschi L, and Sola M. (1999). Effects of nonspecific ion–protein interactions on the redox chemistry of cytochrome *c*. *J Biol Inorg Chem* 4: 601–607, 1999.
25. Benini S, Borsari M, Ciurli S, Dikiy A, and Lamborghini M. Modulation of *Bacillus pasteurii* cytochrome *c*₅₅₃ reduction potential by structural and solution parameters. *J Biol Inorg Chem* 3: 371–382, 1998.

26. Bertrand P, Mbarki O, Asso M, Blanchard L, Guerlesquin F, and Tegoni M. Control of the redox potential in c-type cytochromes *c*: importance of the entropic contribution. *Biochemistry* 34: 11071–11079, 1995.
27. Bond AM. Chemical and electrochemical approaches to the investigation of redox reactions of simple electron transfer metalloproteins. *Inorg Chim Acta* 226: 293–340, 1994.
28. Churg AK, and Warshel A. Control of the redox potential of cytochrome *c* and microscopic dielectric effects in proteins. *Biochemistry* 25: 1675–1681, 1986.
29. Cowan JA. *Inorganic Biochemistry: an Introduction*. New York: Wiley-VCH, 1996.
30. Cusanovich MA, and Caffrey MS. Biological electron transfer: progress and future directions. *Biochim Biophys Acta* 1058: 67–70, 1991.
31. Cutler RL, Davies AM, Creighton S, Warshel A, Moore GR, Smith M, and Mauk AG. Role of arginine-38 in regulation of the cytochrome *c* oxidation–reduction equilibrium. *Biochemistry* 28: 3188–3197, 1989.
32. Döpner S, Hildebrandt P, Rosell FI, and Mauk AG. Alkaline conformational transitions of ferricytochrome *c* studied by resonance Raman spectroscopy. *J Am Chem Soc* 120: 11234–11245, 1998.
33. Dutton PL. Redox potentiometry determination of midpoint potentials of oxidation reduction components of biological electron transfer systems. *Methods Enzymol* 54: 411–434, 1978.
34. Eddowes MJ, and Hill HAO. Novel method for the investigation of the electrochemistry of metalloproteins: cytochrome *c*. *J Chem Soc Chem Commun* 771–772, 1977.
35. Eddowes MJ, and Hill HAO. Electrochemistry of horse heart cytochrome *c*. *J Am Chem Soc* 101: 4461–4464, 1979.
36. Feinberg BA, Liu X, Ryan MD, Schejter A, Zhang C, and Margoliash E. Direct voltammetric observation of redox driven changes in axial coordination and intramolecular rearrangement of the phenylalanine-82–histidine variant of yeast iso-1–cytochrome *c*. *Biochemistry* 37: 13091–13101, 1998.
37. Ferrer JC, Guillemette JG, Bogumil R, Inglis SC, Smith M, and Mauk AG. Identification of Lys79 as an iron ligand in one form of alkaline yeast iso-1–ferricytochrome *c*. *J Am Chem Soc* 115: 7507–7508, 1993.
38. Goldkorn T, and Schejter A. The redox potential of cytochrome *c*-552 from *Euglena gracilis*: a thermodynamic study. *Arch Biochem Biophys* 177: 39–45, 1976.
39. Gopal D, Wilson GS, Earl RA, and Cusanovich MA. Cytochrome *c*: ion binding and redox properties. *J Biol Chem* 263: 11652–11656, 1988.
40. Gray HB, and Ellis WR. Electron transfer. In: *Bioinorganic Chemistry*, edited by Bertini I, Gray HB, Lippard SJ, and Valentine JS. Mill Valley, CA: University Science Books, 1994, pp. 315–363.
41. Gunner MR, Alexov E, Torres E, and Lipovaca S. The importance of the protein in controlling the electrochemistry of heme metalloproteins: methods of calculation and analysis. *J Biol Inorg Chem* 2: 126–134, 1997.
42. Hawkrig FM, and Taniguchi I. The direct electron transfer reactions of cytochrome *c* at electrode surfaces. *Comments Inorg Chem* 17: 163–187, 1995.
43. Heimburg T, and Marsh D. Protein surface-distribution and protein–protein interactions in the binding of peripheral proteins to charged lipid membranes. *Biophys J* 68: 536–546, 1995.
44. Hill HAO, and Hunt NI. Direct and indirect electrochemical investigations of metalloenzymes. *Methods Enzymol* 227: 501–522, 1993.
45. Hong X, and Dixon DW. NMR study of the alkaline isomerization of ferricytochrome *c*. *FEBS Lett* 246: 105–108, 1989.
46. Ikeshoji T, Taniguchi I, and Hawkrig FM. Electrochemically distinguishable states of ferricytochrome *c* and their transition with changes in temperature and pH. *J Electroanal Chem* 270: 297–308, 1989.
47. Jemmerson R, Liu J, Hansauer D, Lam K-P, Mondino A, and Nelson RD. A conformational change in cytochrome *c* of apoptotic and necrotic cells is detected by monoclonal antibody binding and mimicked by association of the native antigen with synthetic phospholipid vesicles. *Biochemistry* 38: 3599–3609, 1999.
48. Kluck RM, Bossy-Wetzel E, Green DR, and Newmayer DD. The release of cytochrome *c* from mitochondria: a primary site for Bcl-2 regulation of apoptosis. *Science* 27: 1132–1136, 1997.
49. Kluck RM, Martin SJ, Hoffman BM, Zhou JS, Green DR, and Newmayer DD. Cytochrome *c* activation of CPP32-like proteolysis plays a critical role in a *Xenopus* cell-free apoptosis system. *EMBO J* 16: 4639–4649, 1997.
50. Koller KB, and Hawkrig FM. Temperature and electrolyte effects on the electron-transfer reactions of cytochrome *c*. *J Am Chem Soc* 107: 7412–7417, 1985.
51. Koller KB, and Hawkrig FM. The effects of temperature and electrolyte at acidic and alkaline pH on the electron transfer reactions of cytochrome *c* at In_2O_3 electrodes. *J Electroanal Chem* 239: 291–306, 1988.
52. Marchon JC, Mashiko T, and Reed CA. How does nature control cytochrome redox potential? In: *Electron Transport and Oxygen Utilization*, edited by Chien H. Amsterdam: Elsevier, 1982, pp. 67–72.
53. Marcus RA, and Sutin N. Electron transfers in chemistry and biology. *Biochim Biophys Acta* 811: 265–322, 1985.
54. Margalit R, and Schejter A. Cytochrome *c*: a thermodynamic study of the relationship among oxidation state, ion-binding and structural parameters. *Eur J Biochem* 32: 492–499, 1973.
55. Mauk AG, and Moore GR. Control of metalloprotein redox potentials: what does site-directed mutagenesis of heme proteins tell us? *J Biol Inorg Chem* 2: 119–125, 1997.
56. Mauk MR, Ferrer JC, and Mauk AG. Proton linkage in formation of the cytochrome *c*-cytochrome *c* peroxidase complex: electrostatic properties of the high- and low-affinity cytochrome binding sites on the peroxidase. *Biochemistry* 33: 12609–12614, 1994.
57. Mignotte B, and Vayessiere J-L. Mitochondria and apoptosis. *Eur J Biochem* 252: 1–15, 1998.

58. Millett F, Miller MA, Green L, and Durham B. Electron transfer between cytochrome *c* and cytochrome *c* peroxidase. *J Bioenerg Biomembr* 27: 341–351, 1995.
59. Moore GR, and Pettigrew GW. *Cytochromes c: Evolutionary, Structural and Physicochemical Aspects*. Berlin: Springer-Verlag; 1990.
60. Moore GR, Harris DE, Leitch FA, and Pettigrew GW. Characterization of ionizations that influence the redox potential of mitochondrial cytochrome *c* and photosynthetic bacterial cytochrome *c*₂. *Biochim Biophys Acta* 764: 331–342, 1984.
61. Osheroff N, Brautigan DL, and Margoliash E. Mapping the anion binding sites on cytochrome *c* by differential chemical modification of lysine residues. *Proc Natl Acad Sci U S A* 77: 4439–4443, 1980.
62. Pelletier H, and Kraut J. Crystal structure of a complex between electron transfer partners, cytochrome *c* peroxidase and cytochrome *c*. *Science* 258: 1748–1755, 1992.
63. Pettigrew GW, and Moore GR. *Cytochromes c: Biological Aspects*. Berlin: Springer-Verlag, 1987.
64. Purring C, Zou H, Wang X, and McLendon G. Stoichiometry, free energy, and kinetic aspects of cytochrome *c*: Apaf-1 binding in apoptosis. *J Am Chem Soc* 121: 7435–7436, 1999.
65. Rafferty SP, Pearce LL, Barker PD, Guillemette JG, Kay CM, Smith M, and Mauk AG. Electrochemical, kinetic, and circular dichroic consequences of mutations at position 82 of yeast iso-1-cytochrome *c*. *Biochemistry* 29: 9365–9369, 1990.
66. Rogers NK. The modeling of electrostatic interactions in the function of globular proteins. *Prog Biophys Mol Biol* 48: 37–66, 1986.
67. Rosell FI, Ferrer JC, and Mauk AG. Proton-linked protein conformational switching: definition of the alkaline conformational transition of yeast iso-1-ferricytochrome *c*. *J Am Chem Soc* 120: 11234–11245, 1998.
68. Sanishvili R, Volz KW, Westbrook EM, and Margoliash E. The low ionic strength crystal structure of horse cytochrome *c* at 2.1 Å resolution and comparison with its high ionic strength counterpart. *Structure* 3: 707–716, 1995.
69. Schejter A, Aviram I, and Goldkorn T. Contribution of electrostatic factors to the oxidation reduction potentials of c-type cytochromes. In: *Electron Transport and Oxygen Utilization*, edited by Chien H. Amsterdam: Elsevier, 1982, pp. 95–99.
70. Scott R, and Mauk AG. *Cytochrome c*. A Multidisciplinary Approach. Sausalito, CA: University Science Books, 1996.
71. Soriano A, Li D, Bian S, Agarwal A, and Cowan JA. Factors influencing redox thermodynamics and electron self-exchange for the [Fe₄S₄] cluster in *Chromatium vinosum* high potential iron protein: the role of core aromatic residues in defining cluster redox chemistry. *Biochemistry* 35: 12479–12486, 1996.
72. Spooner PJ, and Watts A. Reversible unfolding of cytochrome *c* upon interaction with cardiolipin bilayers. 1. Evidence from deuterium NMR measurements. *Biochemistry* 30: 3871–3879, 1991.
73. Spooner PJ, and Watts A. Reversible unfolding of cytochrome *c* upon interaction with cardiolipin bilayers. 2. Evidence from phosphorus-31 NMR measurements. *Biochemistry* 30: 3880–3885, 1991.
74. Spooner PJ, and Watts A. Cytochrome *c* interactions with cardiolipin in bilayers: a multinuclear magic-angle spinning NMR study. *Biochemistry* 31: 10129–10138, 1992.
75. Taler G, Schejter A, Navon G, Vig I, and Margoliash E. The nature of the thermal equilibrium affecting the iron coordination of ferric cytochrome *c*. *Biochemistry* 34: 14209–14212, 1995.
76. Taniguchi I, Iseki M, Eto T, Toyosawa K, Yamaguchi H, and Yasukouchi K. The effect of pH on the temperature dependence of the redox potential of horse heart cytochrome *c* at a bis(4-pyridyl)disulfide-modified gold electrode. *Bioelectrochem Bioenerg* 13: 373–383, 1984.
77. Taniguchi I, Funatsu T, Iseki M, Yamaguchi H, and Yasukouchi K. The temperature dependence of the redox potential of horse heart cytochrome *c* at bis(4-pyridyl)disulfide-modified gold electrode in sodium chloride solutions. *J Electroanal Chem* 193: 295–302, 1985.
78. Tezcan FA, Winkler JR, and Gray HB. Effects of ligation and folding on reduction potentials of heme proteins. *J Am Chem Soc* 120: 13383–13388, 1998.
79. Warshel A, Papazyan A, and Muegge I. Microscopic and semimicroscopic redox calculations: what can and cannot be learned from continuum models? *J Biol Inorg Chem* 2: 143–152, 1997.
80. Yang J, Liu X, Bhalla K, Kim CN, Ibrado AM, Cai J, Peng TI, Jones DP, and Wang X. Prevention of apoptosis by Bcl-2: release of cytochrome *c* from mitochondria blocked. *Science* 275: 1129–1132, 1997.
81. Yee EL, Cave RJ, Guyer KL, Tyma PD, and Weaver MJ. A survey of ligand effects upon the reaction entropies of some transition metal redox couples. *J Am Chem Soc* 101: 1131–1137, 1979.
82. Zhou H-X. Effects of mutations and complex formation on the reduction potentials of cytochrome *c* and cytochrome *c* peroxidase. *J Am Chem Soc* 116: 10362–10375, 1994.
83. Zhou JS, and Hoffman BM. Stern-Volmer in reverse: 2:1 stoichiometry of the cytochrome *c*-cytochrome *c* peroxidase electron-transfer complex. *Science* 265: 1693–1696, 1994.

Address reprint requests to:

Prof. Marco Sola
Department of Chemistry
University of Modena and Reggio Emilia
Via Campi 183
41100 Modena, Italy

E-mail: sola@unimo.it

Received for publication August 1, 2000; accepted November 10, 2000.

This article has been cited by:

1. Zhiyong Guo, Huina Zhang, Panpan Gai, Jing Duan. 2011. Direct electrochemistry of cytochrome c entrapped in agarose hydrogel by protein film voltammetry. *Russian Journal of Electrochemistry* **47**:2, 175-180. [[CrossRef](#)]
2. Giorgio Zoppellaro, Kara L. Bren, Amy A. Ensign, Espen Harbitz, Ravinder Kaur, Hans-Petter Hersleth, Ulf Ryde, Lars Hederstedt, K. Kristoffer Andersson. 2009. Review: Studies of ferric heme proteins with highly anisotropic/highly axial low spin ($S = 1/2$) electron paramagnetic resonance signals with bis-Histidine and histidine-methionine axial iron coordination. *Biopolymers* **91**:12, 1064-1082. [[CrossRef](#)]
3. Stefano Monari, Gianantonio Battistuzzi, Marco Borsari, Diego Millo, Cees Gooijer, Gert Zwan, Antonio Ranieri, Marco Sola. 2008. Thermodynamic and kinetic aspects of the electron transfer reaction of bovine cytochrome c immobilized on 4-mercaptopyrindine and 11-mercapto-1-undecanoic acid films. *Journal of Applied Electrochemistry* **38**:7, 885-891. [[CrossRef](#)]
4. Manon J. W. Ludden, Jatin K. Sinha, Gunther Wittstock, David N. Reinhoudt, Jurriaan Huskens. 2008. Control over binding stoichiometry and specificity in the supramolecular immobilization of cytochrome c on a molecular printboard. *Organic & Biomolecular Chemistry* **6**:9, 1553. [[CrossRef](#)]
5. G. Battistuzzi, M. Bellei, M. Borsari, G. Di Rocco, A. Ranieri, M. Sola. 2005. Axial ligation and polypeptide matrix effects on the reduction potential of heme proteins probed on their cyanide adducts. *JBIC Journal of Biological Inorganic Chemistry* **10**:6, 643-651. [[CrossRef](#)]
6. J Haddad. 2004. Redox and oxidant-mediated regulation of apoptosis signaling pathways: immuno-pharmaco-redox conception of oxidative siege versus cell death commitment. *International Immunopharmacology* **4**:4, 475-493. [[CrossRef](#)]